A Curvature Response Model for Weak-Field Gravity

Jack Pickett – 28th March 2026

1. Abstract

Observations of galaxy rotation curves, cluster dynamics, and gravitational collapse reveal systematic deviations from predictions based on a strictly Newtonian inverse-square gravitational response when only baryonic matter is considered. These discrepancies are conventionally addressed by introducing non-baryonic dark matter components.

This work develops an alternative interpretation in which the weak-field gravitational response of spacetime depends on the local baryonic environment. Starting from a modified gravitational action, an environment-weighted generalisation of the Poisson equation is derived, introducing a spatially varying response coefficient $\mu(r)$. In the weak-field limit, this formulation yields an exponential gravitational potential, characterised by a curvature-response parameter $\kappa(r)$ that emerges directly from the field equation.

A phenomenological parameterisation of κ in terms of baryonic density and velocity shear is introduced and evaluated against the SPARC galaxy rotation-curve dataset. The model reproduces the observed sub-linear acceleration relation without requiring additional matter components. The same global parameter set yields consistent behaviour across multiple regimes, including galactic discs, cluster environments, and gravitational collapse.

These results suggest that part of the observed discrepancy between baryonic mass and gravitational dynamics arises from modelling gravitational response as a fixed, local function rather than an environment-dependent process. The framework provides a geometric description in which curvature responds to baryonic organisation, rather than being determined solely by local mass: offering a unified description of gravitational behaviour across a range of structured astrophysical systems.

2. Literature Context

Alternative approaches to gravitational anomalies can be understood in terms of how they modify the Newtonian Poisson equation,

$$\nabla^2\Phi = 4\pi G\rho$$

In the standard dark-matter interpretation the equation itself is unchanged, but the source term is extended to include an additional non-baryonic component [Navarro1997, Clowe2006, Planck2018],

$$\nabla^2\Phi = 4\pi G\left(\rho_b + \rho_{\mathrm{DM}}\right)$$

so that the observed dynamics arise from an effective mass distribution rather than baryonic matter alone.

Phenomenological departures from Newtonian dynamics, typified by MOND [Milgrom1983, Famaey2012], instead modify the relation between the potential and the baryonic source

by introducing an acceleration-dependent response function μ,

$$\nabla \cdot \left[\mu\left(\frac{|\nabla \Phi|}{a_0} \right) \nabla \Phi \right] = 4\pi G \rho_b$$

which reduces to the Newtonian form when μ → 1. Relativistic extensions such as TeVeS embed this behaviour within additional fields [Bekenstein2004].

Entropic and emergent-gravity proposals, including Verlinde's 2017 framework, similarly reinterpret the gravitational response as arising from collective degrees of freedom, leading to effective modifications of the relation between acceleration and baryonic matter [Verlinde2017].

Parallel work in modified curvature theories alters the gravitational action itself, replacing the Einstein-Hilbert term R with a nonlinear function f(R), leading to modified field equations of the form

$$f'(R)R_{\mu\nu} - \frac{1}{2}f(R)g_{\mu\nu} - \nabla_\mu \nabla_\nu f'(R) + g_{\mu\nu}\Box f'(R) = 8\pi G\, T_{\mu\nu}$$

and corresponding deviations from Newtonian behaviour in the weak-field limit [DeFelice2010, Cognola2008].

These frameworks differ in mechanism with additional source terms, acceleration-dependent response functions, or modified curvature invariants, but share a common structural feature: the gravitational response is prescribed as a fixed functional dependence on mass-energy or acceleration scale.

However, real astrophysical systems are not characterised by isolated sources, but by structured, many-body environments in which density gradients, velocity shear, and large-scale organisation play a central role. In such systems, gravitational behaviour is inferred from motion within an extended curvature background rather than from pairwise interactions alone.

This suggests that part of the observed discrepancy may arise not from missing mass or fixed modifications to the force law, but from how the gravitational response is modelled in complex environments. Rather than prescribing a fixed functional form, the present framework explores a formulation in which the effective curvature response depends explicitly on local environmental properties, allowing gravitational behaviour to emerge from the structure of the baryonic distribution itself.

This reframes the problem from modifying gravitational laws to modelling how curvature propagates through structured baryonic environments and motivates a formulation in which the gravitational response, although not prescribed a priori, emerges from the structure of the local baryonic environment. The following section develops this framework starting from a modified Poisson description.

3. Environmental Curvature Response

The framework reframes gravitational dynamics as a response of spacetime to structured baryonic environments as opposed to a fixed interaction determined solely by local mass. The Newtonian Poisson equation provides the simplest relation between mass distribution and gravitational potential in the weak-field limit. In its standard form, it assumes that the gravitational response of spacetime is linear and universal. However, in structured astrophysical systems, this assumption may be too restrictive:

the observed gravitational behaviour reflects motion within an extended curvature environment rather than a purely local response to mass density.

This suggests that, rather than modifying the source term or introducing additional fields, a natural generalisation is to allow the response itself to vary with environment. This can be achieved by introducing a spatially varying response coefficient μ, leading to a modified Poisson equation.

3.1. Environment-Weighted Poisson Response

To capture this behaviour while preserving the standard weak-field structure, an environment-weighted Poisson equation can be motivated as the weak-field limit of a covariant modified-gravity action

$$S = \int \sqrt{-g}[R\exp(\alpha R) + 16\pi G L_m], d^4x$$

where variation with respect to the metric yields modified field equations of $f(R)$ type. In systems with approximate spherical or disc symmetry, the scalar curvature R varies smoothly with radial position and can be treated as a slowly varying function of r. In the weak-field regime, this permits a local expansion in which curvature-dependent corrections may be expressed as an effective radial response factor, leading to an exponential parametrisation in r at leading order.

In the static, low-curvature limit these equations reduce to the generalised Poisson form

$$\nabla \cdot (\mu \nabla \Phi) = 4\pi G \rho,$$

with response coefficient $\mu(r) = \exp(-\kappa r)$ serving as an effective parametrisation of the curvature response. Because the field equations are derived from a diffeomorphism-invariant action, the twice-contracted Bianchi identities guarantee local conservation of the stress-energy tensor,

$$\nabla_\mu T^{\mu\nu} = 0,$$

with modifications arising from curvature-dependent terms rather than additional matter sources.

Writing the gravitational acceleration as

$$\mathbf{g} = -\nabla \Phi,$$

the field equation becomes

$$\nabla \cdot (\mu \mathbf{g}) = -4\pi G \rho.$$

For a spherically symmetric configuration outside the main baryonic mass distribution, where the enclosed mass $M(r)$ varies slowly, integration yields

$$r^2 \mu(r) g(r) = G M(r).$$

The effective gravitational acceleration is therefore

$$g(r) = \frac{G M(r)}{r^2 \mu(r)}.$$

The κ-framework expresses this response through an exponential curvature factor

$$g(r) = g_N(r)\, e^{\kappa(r) r},$$

where $g_N(r) = GM(r)/r^2$ is the Newtonian acceleration. Equating the two forms gives

$$\mu(r) = e^{-\kappa(r) r},$$

which implies

$$\kappa(r) = -\frac{1}{r} \ln \mu(r).$$

The quantity κ therefore represents the local logarithmic response rate of the environment-weighted gravitational field. This formulation preserves the Newtonian limit and conservation of gravitational flux while allowing the effective gravitational response to vary with environmental structure.

3.2. Effective Potential

While the modified field equation defines how curvature responds to the environment, observable dynamics are determined by the resulting acceleration field. Therefore it is necessary to express this response in terms of an effective potential and acceleration explicitly. In the weak-field regime, gravitational motion is determined by the gradient of the potential. The environment-weighted response therefore translates directly into a modified acceleration field. From the field equation, the gravitational acceleration follows as

$$g = -\nabla \Phi.$$

In regions outside the dominant baryonic mass distribution, this leads to an effective (weak-field) gravitational potential of the form

$$\Phi_{\text{eff}}(r) = -\frac{GM}{r}\, e^{\kappa(r)\, r}$$

which produces the radial acceleration

$$g_{\text{eff}}(r) = \frac{GM}{r^2}\, e^{\kappa(r)\, r}$$

The circular velocity in an axisymmetric system follows from

$$v_\kappa(r) = \sqrt{\frac{GM(r)}{r}}\, e^{\kappa(r)\, r/2}$$

These expressions determine the gravitational behaviour throughout this work and hold to leading order in the limit where $\kappa(r)$ varies slowly with radius.

3.3. Curvature-Response Coefficient

The curvature-response coefficient κ, defined via $\mu(r) = e^{-\kappa(r) r}$, is not specified a priori by the field equation. The field equation determines how curvature responds to the environment but does not uniquely specify how this response depends on the detailed baryonic structure. A phenomenological parameterisation is therefore introduced $\kappa(\rho, r)$ as a scalar quantity that reflects the influence of a local matter environment on the extension of gravitational curvature. The coefficient depends on two measurable properties of the environment: the mass density ρ and the radial velocity shear $\partial v/\partial r$. The functional form is

$$\kappa(\rho, r) = \kappa_0 + k_v \left(\frac{\partial v/\partial r}{10^{-12}\,\mathrm{s}^{-1}} \right)^3 \left(\frac{\rho}{\rho_0} \right)^{1/2}$$

and reflects a nonlinear sensitivity to local dynamical structure through velocity shear, modulated by the ambient mass density. The parameters have the following roles:

- κ_0 sets a background curvature scale.
- k_v sets the magnitude of the shear-response contribution.
- ρ_0 defines the density scale at which the curvature response transitions between regimes.

These quantities are held constant across all applications in this study. Their values are

$$\kappa_0 = 2.6 \times 10^{-26}\,\mathrm{m}^{-1},\ k_v = 5 \times 10^{-26}\,\mathrm{m}^{-1},\ \rho_0 = 1600\,\mathrm{kg\,m}^{-3}$$

3.4. Behaviour Across Regimes

The form of $\kappa(\rho, r)$ yields four natural regimes of gravitational behaviour.

- Solar-System Regime
  Local densities are high and the radial velocity shear is small. The product κr remains much smaller than unity and the effective acceleration approaches GM/r^2 to high precision. Standard planetary dynamics are recovered.
- Galactic Regime
  Densities decrease with radius while coherent differential rotation produces increasing shear. The curvature-response term becomes significant at large radii. The effective velocity profile maintains an extended form through the exponential factor $e^{\kappa r/2}$, generating characteristic flat rotation curves.
- Cluster and Collision Regime
  Galaxy clusters and interacting systems display strong velocity gradients and intermediate densities. These environments produce large curvature-response values and enhanced gravitational lensing magnitudes. The scalar κ field reaches its largest observational values in these systems.
- Cosmological Regime
  On scales where density gradients and internal shear are negligible, the background component κ_0 dominates. The corresponding acceleration scale $a_\kappa = \kappa_0 c^2$ establishes a uniform curvature contribution that influences late-time expansion.

3.5. Parameter Scales

The density scale $\rho_0 = 1600\,\mathrm{kg\,m}^{-3}$ corresponds to densities characteristic of planetary interiors and provides a reference from which galactic and cluster densities differ by many orders of magnitude. The shear reference scale $10^{-12}\,\mathrm{s}^{-1}$ is representative of differential rotation gradients in the outer regions of spiral galaxies. The background curvature scale κ_0 corresponds to an acceleration of magnitude $a_\kappa = \kappa_0 c^2 \approx 10^{-9}\,\mathrm{m\,s}^{-2}$, comparable to the empirical acceleration scale associated with large-scale structure flows.

3.6. Practical Evaluation

The density $\rho(r)$ and velocity gradient $\partial v/\partial r$ are obtained from observationally inferred baryonic mass distributions and measured or modelled rotation profiles. These quantities determine $\kappa(r)$ throughout a system. The curvature-modified potential and

acceleration follow directly from the expressions above. Once $\kappa(r)$ is computed, no additional assumptions or system-specific parameters are introduced.

4. Observational Predictions and Results

The environment-dependent curvature formulation produces measurable deviations from Newtonian behaviour only in regimes where baryonic density declines and velocity shear becomes non-negligible. A single global parameter set is applied across all systems considered below, allowing direct comparison between planetary and galactic environments.

4.1. Solar-System Regime

In the Solar System, both baryonic density and velocity shear remain small, suppressing the curvature-response parameter κ. In this limit, the effective gravitational acceleration reduces to

$$g(r) \simeq \frac{GM}{r^2}$$

with corrections from the exponential curvature term remaining well below current observational sensitivity.

To test this explicitly, high-precision N-body integrations were performed using the REBOUND IAS15 integrator across a 200-year baseline. Simulations include the Sun and the eight major planets, with orbital diagnostics computed relative to a Newtonian baseline. The κ-framework introduces a perturbative correction dependent on environmental density and strain. For Solar System conditions, the density is fixed at

$$\rho = 10^{-12}\,\mathrm{kg\,m^{-3}}$$

while the strain-rate parameter is varied to explore dynamical response.

4.1.1. Orbital Behaviour

Across all simulations in the weak-strain regime, orbital structure remains essentially unchanged:

- $\Delta a \lesssim 10^{-11}\,\mathrm{AU},$
- $\Delta e \lesssim 10^{-10}$

indicating negligible deformation of Keplerian orbits.

However, a small but systematic secular drift in perihelion orientation is observed. For representative parameter values,

- Mercury: ~0.03 arcsec per century
- Earth: ~0.05 arcsec per century
- Jupiter: ~0.13 arcsec per century

Two independent estimators (orbital elements and the Laplace-Runge-Lenz (LRL) vector) agree closely, confirming the robustness of the signal.

4.1.2. Dynamical Regimes

Parameter sweeps reveal three distinct regimes:

- Stable regime: negligible deviations, effectively Newtonian
- Distorted regime: increasing apsidal motion with mild orbital deformation
- Unstable regime: orbital divergence and breakdown of coherent motion

The Solar System resides firmly within the stable regime, with measurable precession appearing well before any structural instability.

These results demonstrate that the κ–framework acts as a weak perturbative correction in high–density environments, preserving established Solar System constraints while introducing a distinct dynamical signature.

4.1.3. Figures

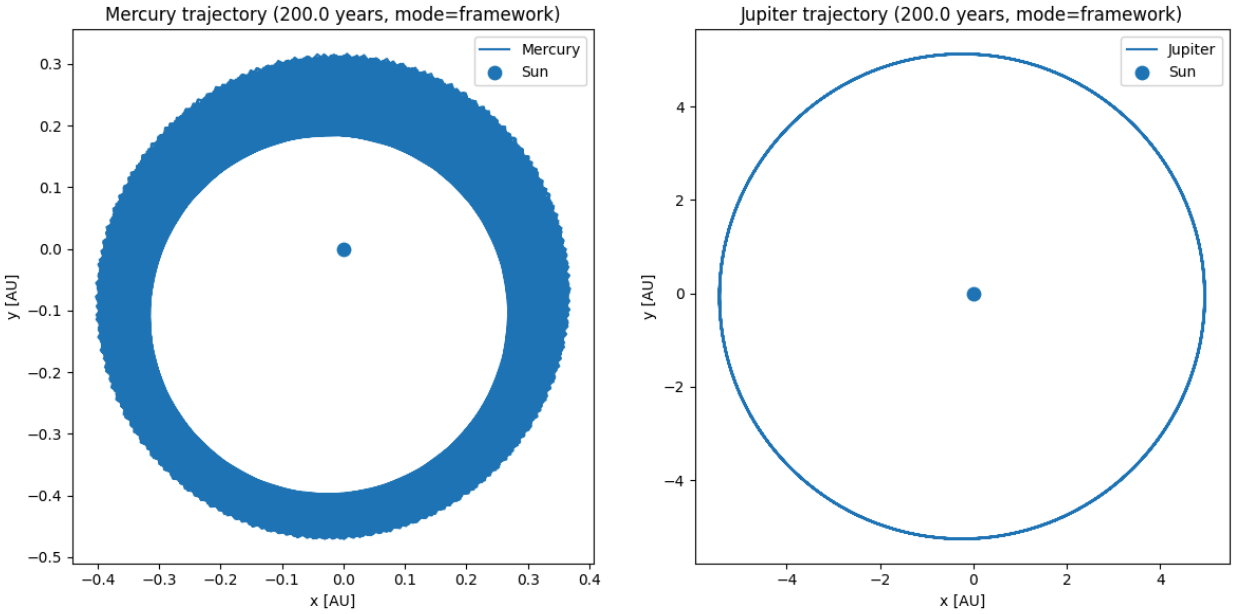

Figures 1 & 2: Newtonian baseline integration of representative planetary orbits using the REBOUND IAS15 integrator. Mercury (inner orbit) and Jupiter (outer orbit) illustrate the range of orbital scales and eccentricities present in the planetary Solar System. The simulations remain dynamically stable over the 200–year integration period.

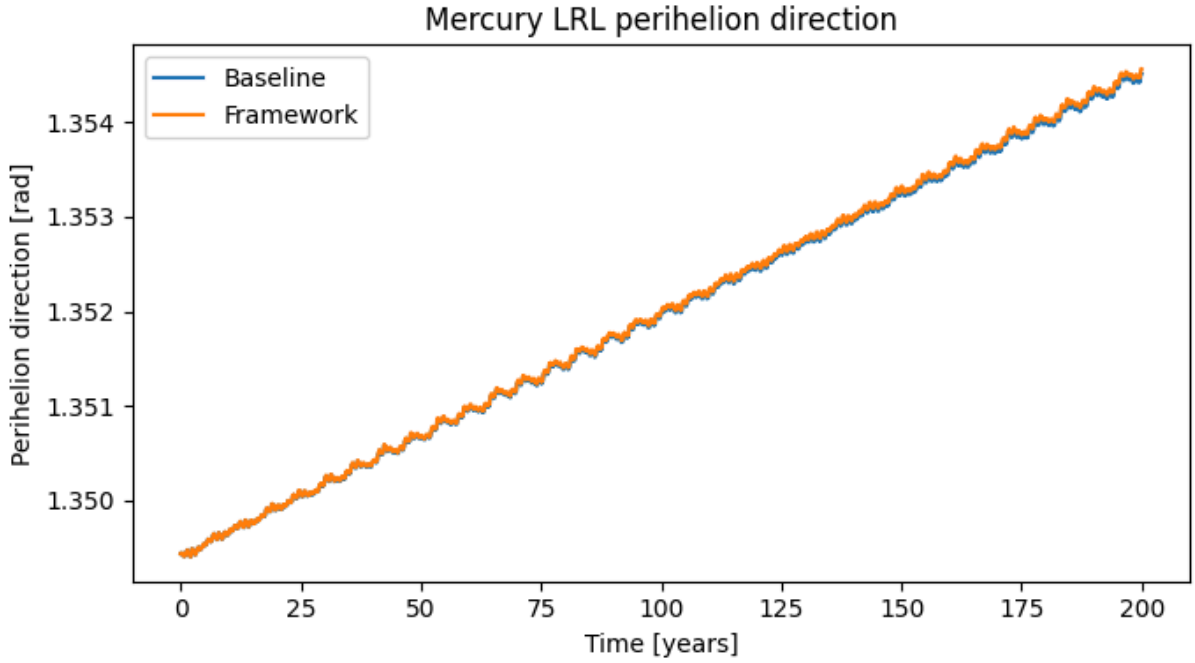

Figure 3: Mercury perihelion direction comparison: Comparison of the perihelion direction inferred from the Laplace–Runge–Lenz (LRL) vector for the Newtonian baseline and the κ–framework simulation over a 200–year integration. The near overlap of the two curves indicates that the κ perturbation produces only a very small secular deviation from the Newtonian orbital orientation.

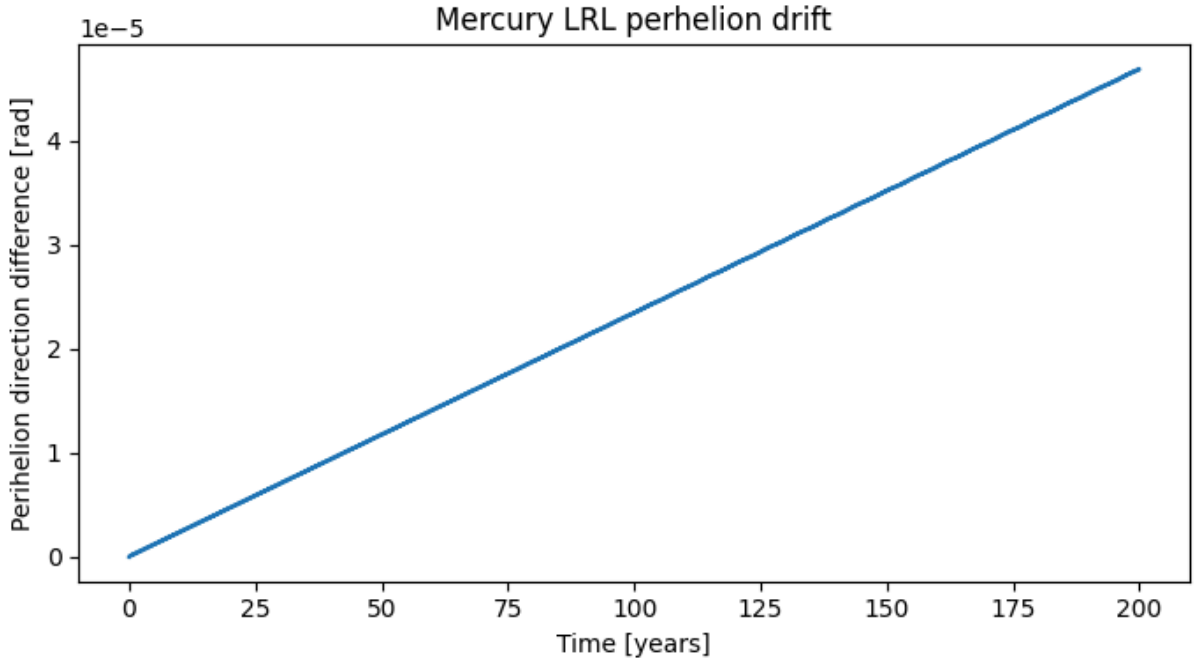

Figure 4: Secular perihelion drift of Mercury: Accumulated difference in the perihelion direction derived from the LRL vector between the Newtonian baseline and the κ–framework simulation. The ~linear trend indicates a slow secular rotation of the orbital ellipse while the overall orbital structure remains essentially unchanged

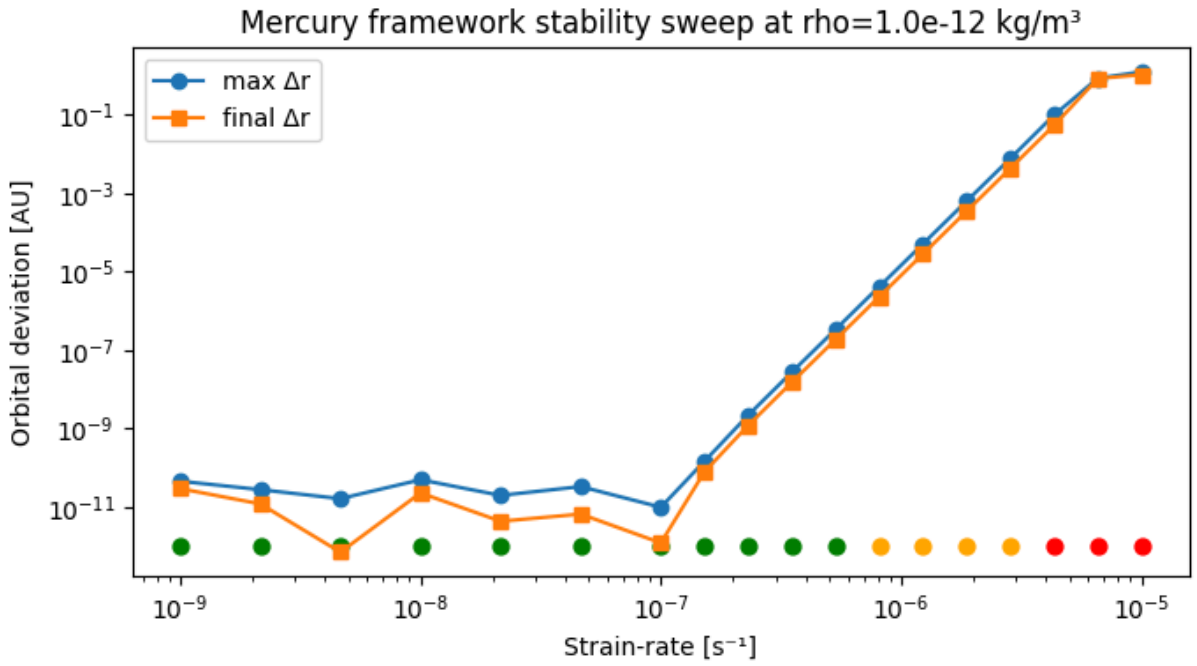

Figure 5: Mercury orbital deviation as a function of environmental strain-rate: Maximum and final orbital deviation relative to the Newtonian baseline for Mercury over a 200-year integration. Three dynamical regimes are visible: a stable regime in which orbital deviations remain negligible, a transitional regime with increasing perturbation, and an unstable regime in which the orbit diverges. The onset of measurable dynamical deviation occurs well after the weak-perturbation regime explored in the present Solar System tests.

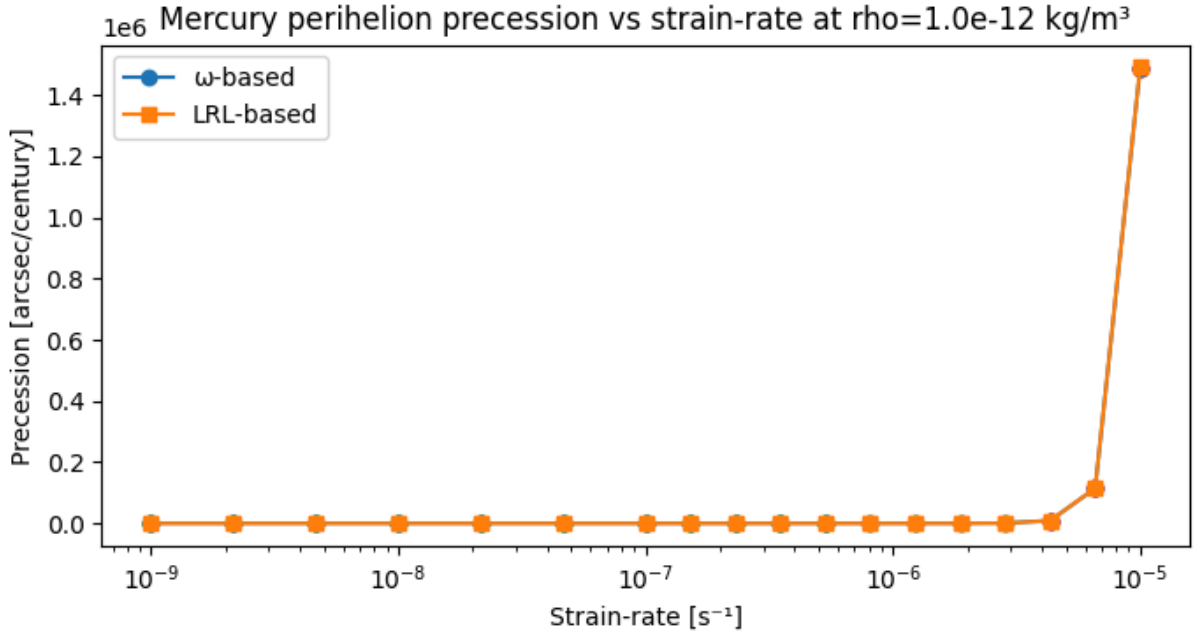

Figure 6: Mercury perihelion precession as a function of environmental strain-rate: Estimated perihelion precession rate for Mercury derived from both the angular momentum (ω-based) method and the Laplace-Runge-Lenz (LRL) vector method as a function of the κ-framework strain-rate parameter for a fixed density $\rho = 10^{-12}\,\mathrm{kg\,m^{-3}}$. In the low-strain regime relevant to Solar System conditions, the predicted precession remains extremely small and the two independent diagnostics agree closely. Rapid growth in precession occurs only when the strain-rate approaches values where the orbital solution itself becomes dynamically unstable.

4.2. Spiral–Galaxy Rotation Curves (SPARC)

In galactic environments, baryonic density declines and velocity shear becomes significant, allowing the curvature–response term to contribute appreciably.

The κ–framework modifies the Newtonian velocity field as

$$v_{\rm obs}(r) = v_N(r)\exp\left(\frac{\kappa(r)\,r}{2}\right)$$

where $v_N(r)$ is the baryonic Newtonian circular velocity.

4.2.1. Empirical Determination of κ

Given observed and baryonic velocities, κ can be inferred directly:

$$\frac{\kappa(r)\,r}{2} = \ln\left(\frac{v_{\rm obs}}{v_N}\right)$$

This quantity represents the logarithmic amplification of the baryonic velocity field.

Using the SPARC dataset, empirical values of κ are computed across ~170 galaxies spanning a wide range of masses and morphologies.

4.2.2. Environmental Correlations

Stacking measurements across the SPARC sample reveals a clear correlation between κ and baryonic acceleration:

$$g_{\rm bar} = \frac{v_N^2}{r}$$

The empirical relation is well described by

$$\frac{\kappa r}{2} = a + b\,\log_{10}(g_{\rm bar})$$

with an extended model including shear

$$\frac{\kappa r}{2} = a + b\,\log_{10}(g_{\rm bar}) + c\,\log_{10}\left(\frac{dv}{dr}\right)$$

These relations are obtained through regression on training subsets and evaluated across held–out galaxies.

4.2.3. Rotation Curve Reconstruction

Predicted velocities are then computed as

$$v_{\rm pred} = v_N\exp\left(\frac{\kappa r}{2}\right)$$

Across repeated train/test splits, the κ–based model improves fits relative to baryons–only Newtonian predictions for approximately 85–90% of galaxies.

The inclusion of baryonic shear provides a modest additional improvement.

4.2.4. Radial Acceleration Relation

The κ–framework naturally reproduces the observed radial acceleration relation (RAR), defined by

$$g_{\rm obs} = \frac{v_{\rm obs}^2}{r}$$

Residual diagnostics show that κ–based predictions closely track the observed RAR trend, with residuals concentrated near zero and reduced scatter when shear is included.

4.2.5. Figures

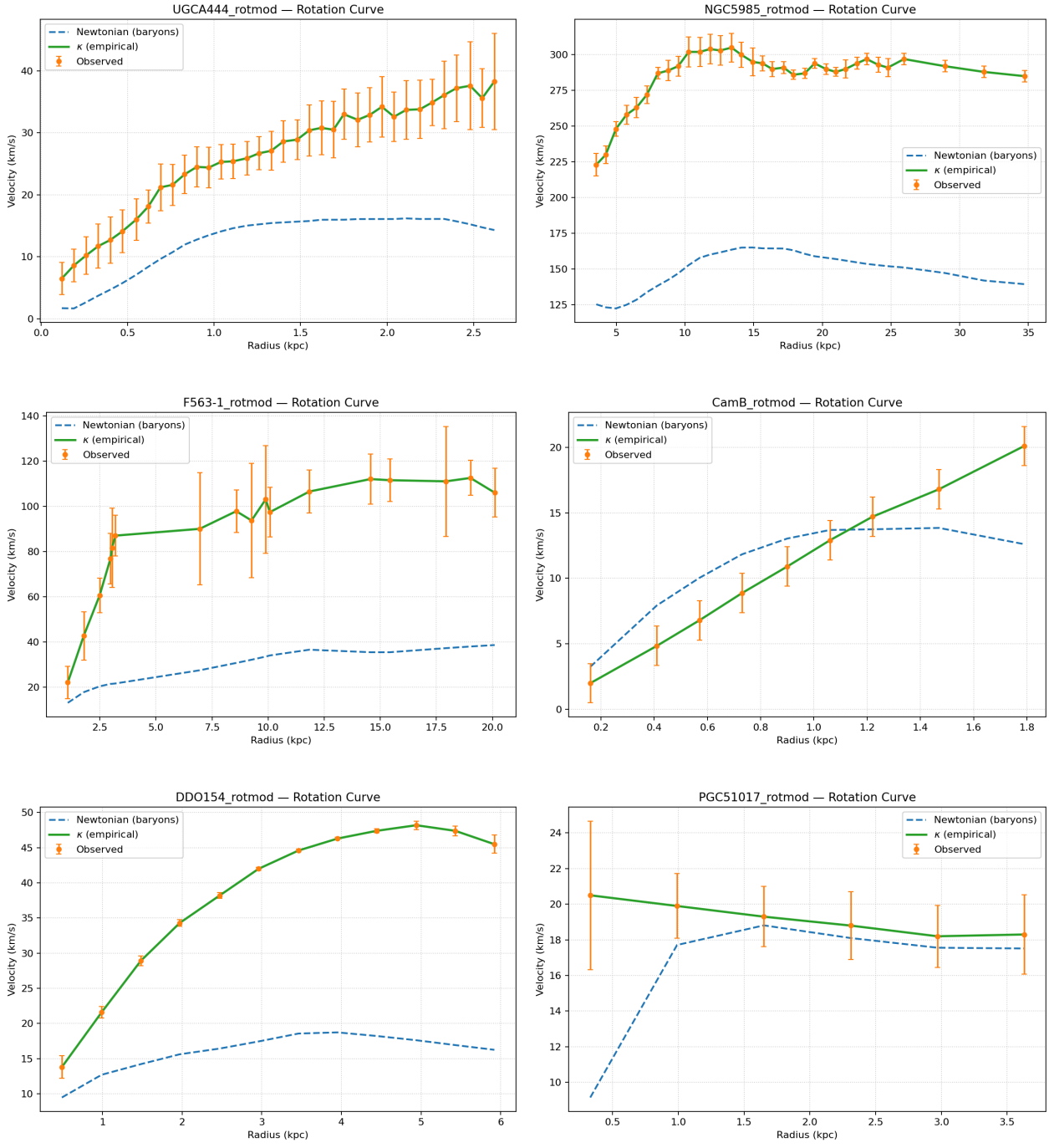

Figures 7–12: show representative rotation curves from the SPARC sample, including the baryonic Newtonian prediction, the observed velocities, and the κ–framework reconstruction.

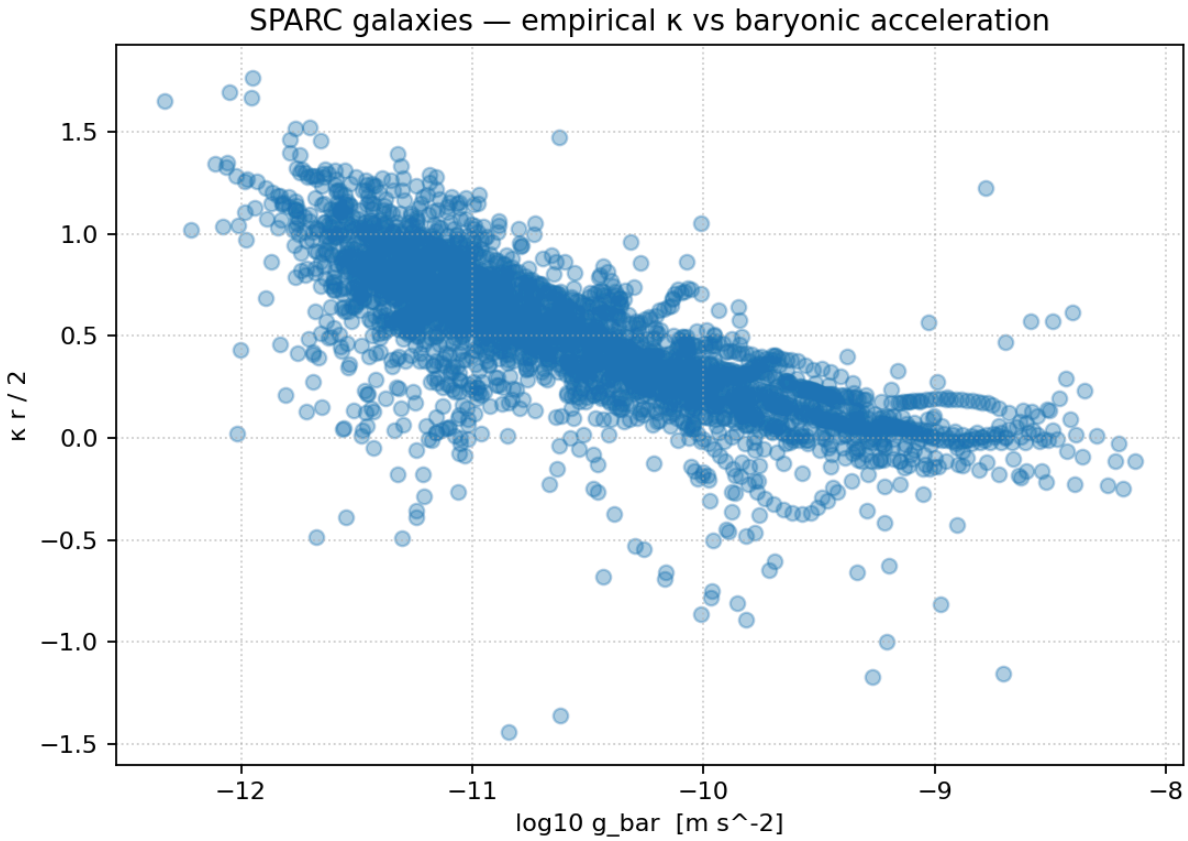

Figure 13: reveals a clear correlation between κr/2 and baryonic acceleration across the stacked SPARC sample.

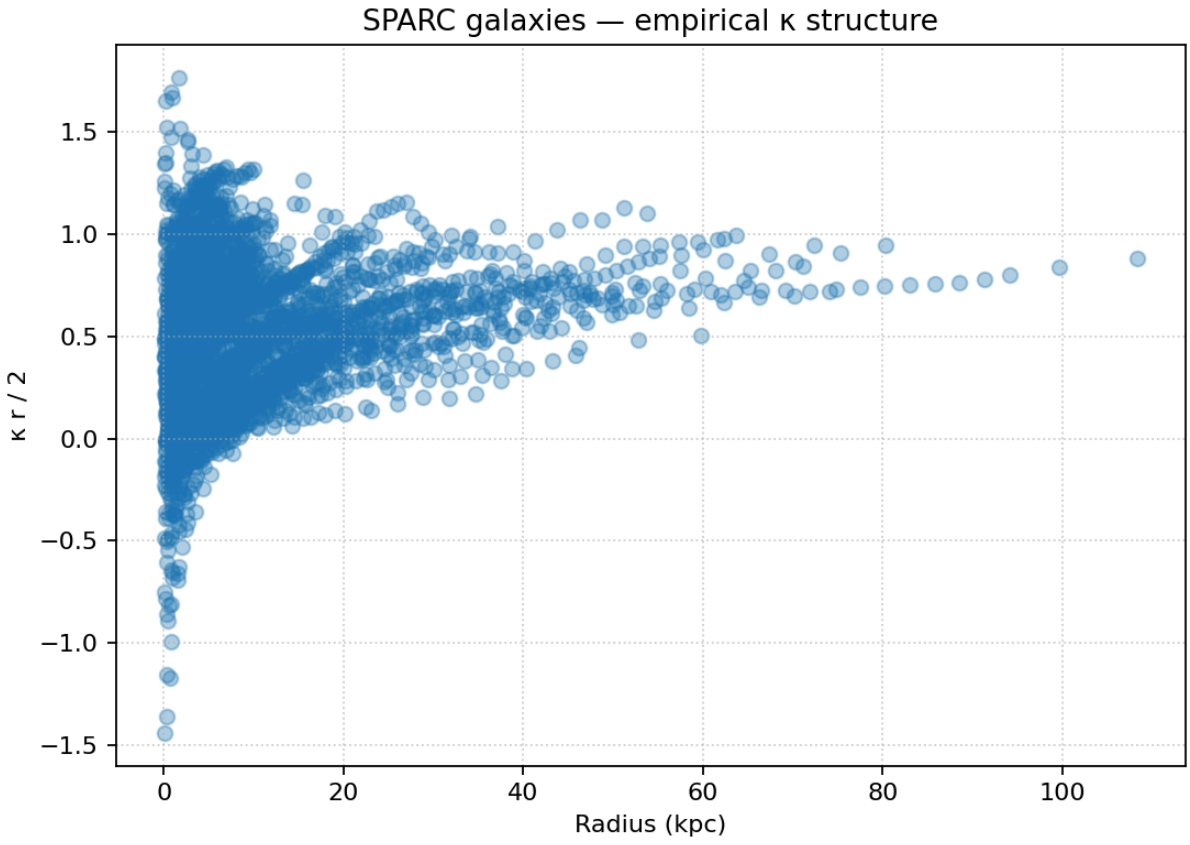

Figure 14: Empirical κ structure across the SPARC sample. Each point represents a measurement of κr/2 at a radius within a galaxy.

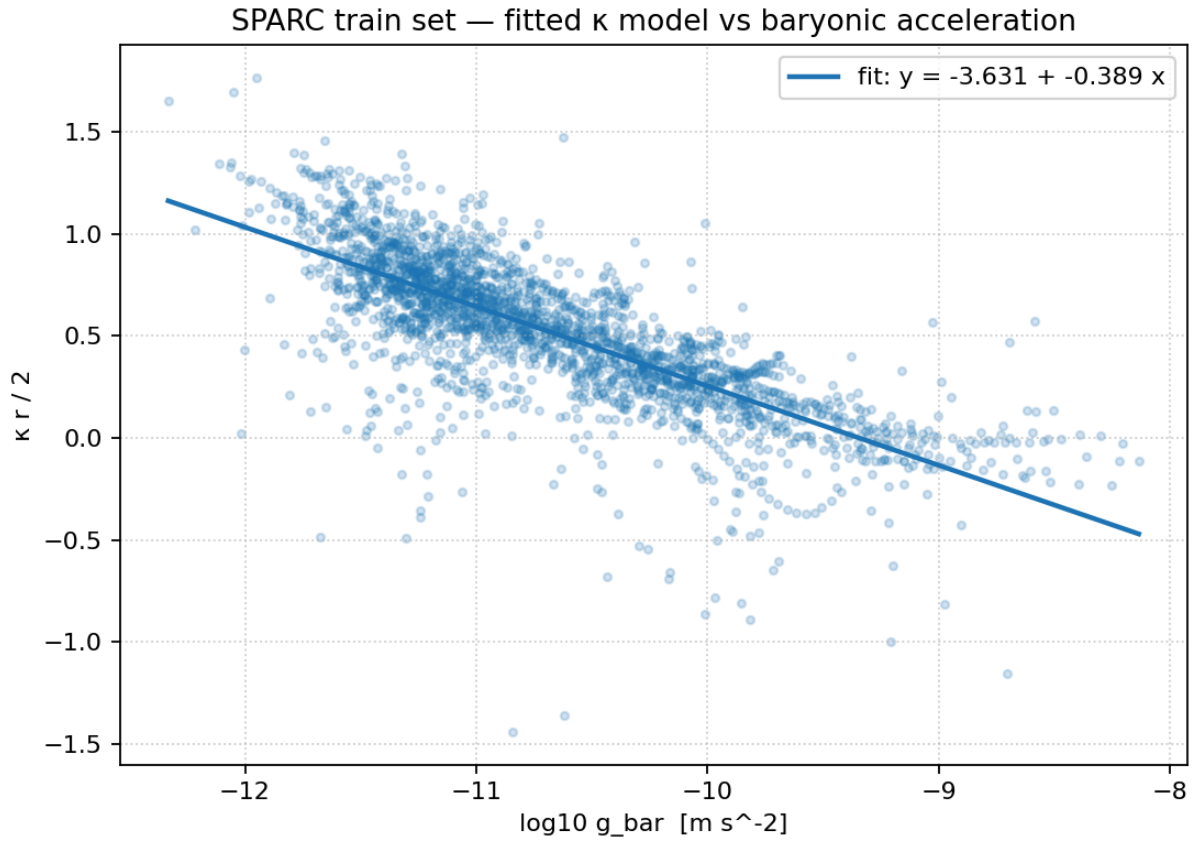

Figure 15: Linear regression fit describing the empirical relation between κr/2 and baryonic acceleration.

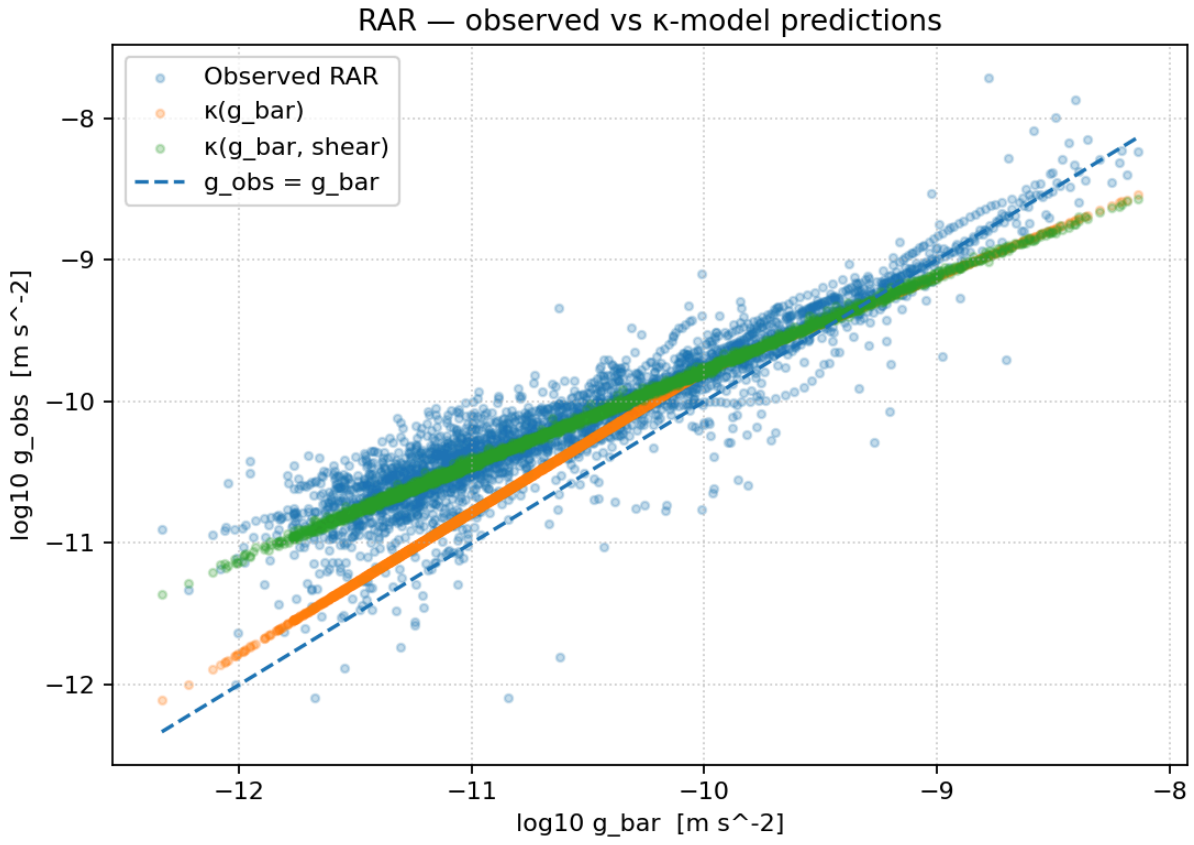

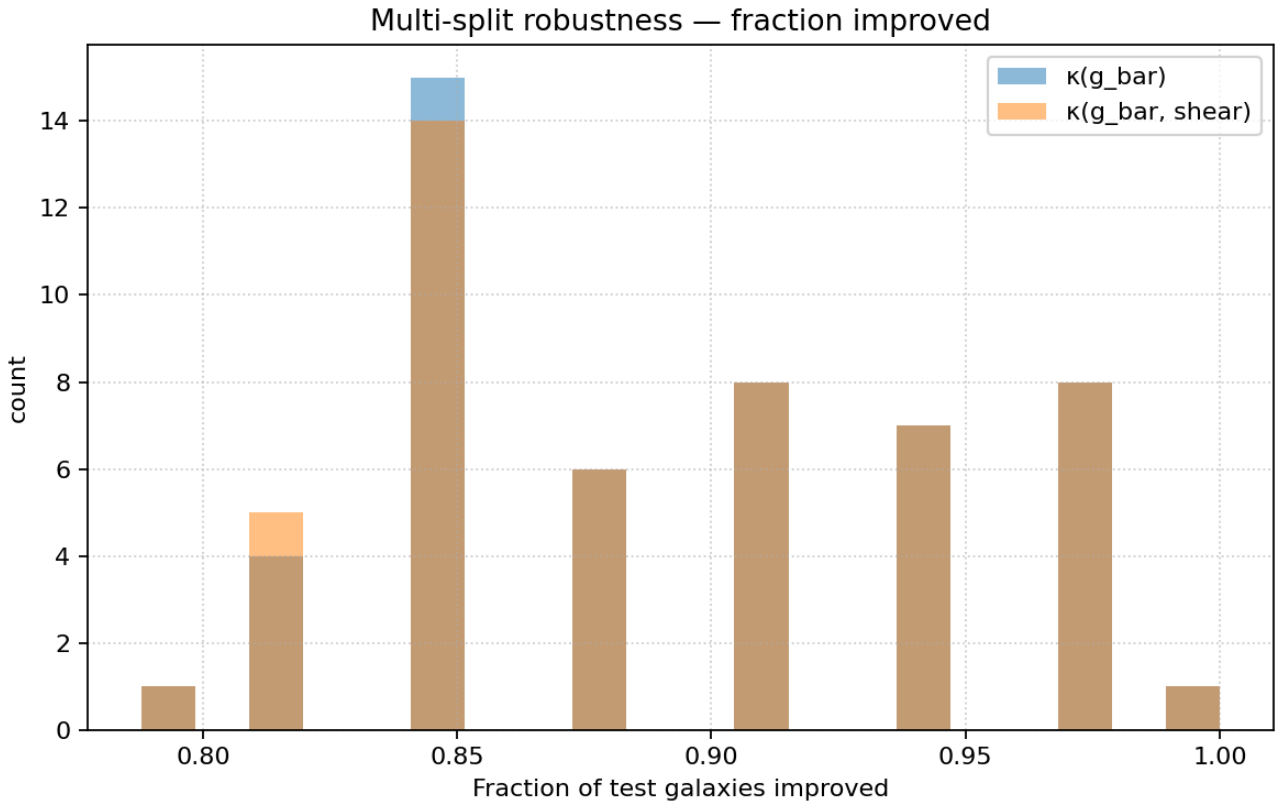

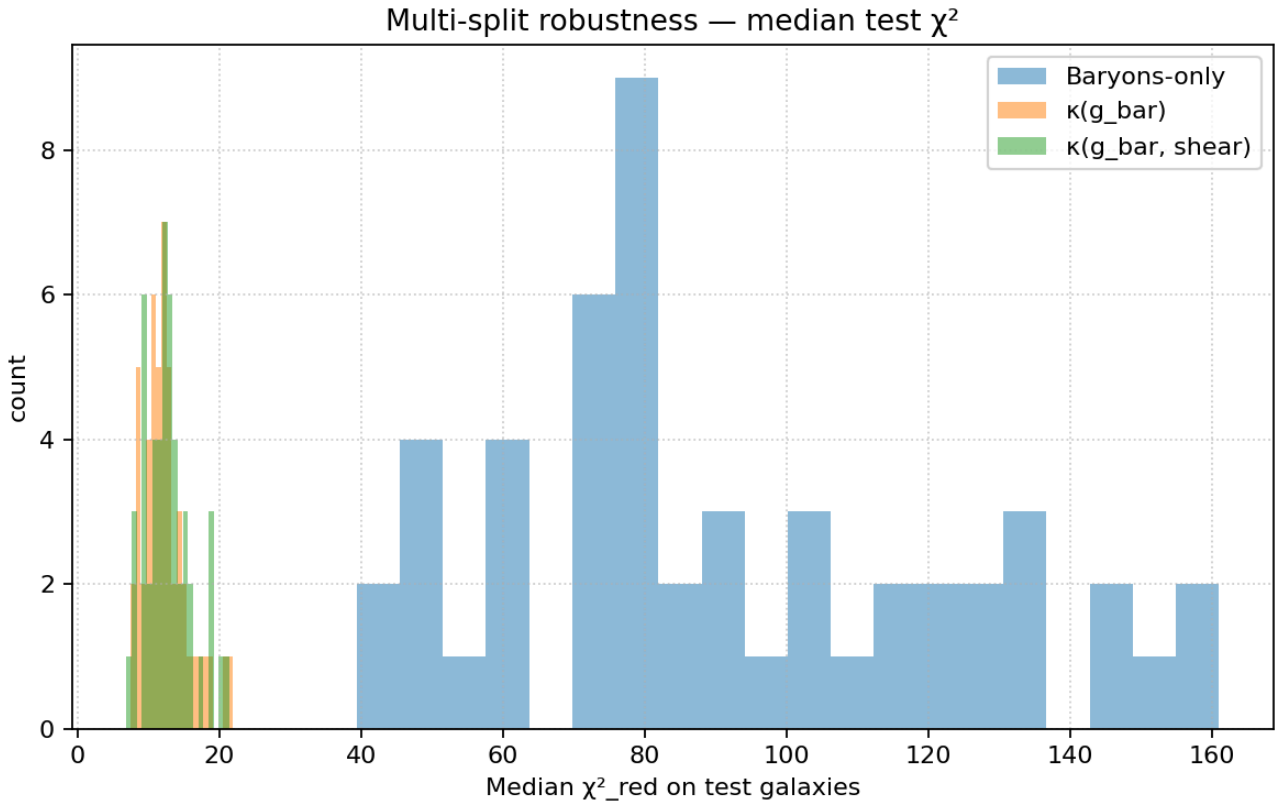

Figures 16–18: Comparison between κ–framework predictions and the observed radial acceleration relation.

These results demonstrate that a simple environmental parameterisation of κ captures a substantial fraction of the rotation-curve discrepancy without introducing additional mass components.

4.3. Behaviour Across Regimes

The κ–framework exhibits a continuous transition across gravitational environments:

- High–density / low–shear (Solar System):
  $\kappa \to 0$, Newtonian behaviour recovered
- Intermediate regime (galaxies):
  κ grows with declining density and increasing shear, producing flat rotation curves
- High–response regime (collapse):
  κ becomes large, enhancing effective gravitational attraction

The key feature is that deviations from Newtonian behaviour arise not from additional mass components, but from an environment–dependent amplification of curvature.

4.4. Summary of Observational Behaviour

Across both regimes:

- Solar System dynamics remain stable with only weak secular signatures
- Galaxy rotation curves are reproduced without dark matter halos
- The same functional form of κ applies across systems
- Observed scaling relations emerge naturally from environmental dependence

Taken together, these results indicate that a curvature response dependent on baryonic environment can provide a unified description of gravitational behaviour across astrophysical systems.

5. Astrophysical Implications

5.1. Disc Formation and Early Disc Stability

Disc galaxies present challenges for ΛCDM–based structure formation where simulations generically produce excessive angular momentum loss "catastrophic cooling", thick discs, and delayed disc formation, with thin, rotation–supported discs emerging only under finely tuned feedback prescriptions.

In the κ–framework, the same environmental curvature term that flattens rotation curves also reshapes the collapse pathway of protogalactic gas. In a collapsing, rotating cloud, baryonic density increases fastest along the minor axis, and the shear grows rapidly as rotation proceeds. Because κ depends on both density and shear, the κ –field develops an oblate profile early in the collapse, steepening curvature in the plane of rotation relative to the vertical direction.

This produces two immediate consequences:

1. Planar collapse is preferentially reinforced.
   The curvature gradient generated by κ accelerates infall toward the rotation plane, driving disc formation without requiring angular momentum loss to be suppressed.

2. Vertical support is enhanced.
   Because κ decreases with radius but increases with density, the disc plane becomes the locus of maximum curvature, inhibiting thick-disc growth and stabilising the thin-disc structure earlier than in Newtonian dynamics.

These effects appear at exactly the radii and densities associated with observed high-redshift disc galaxies. In this view, disc formation is not delayed or finely tuned; it is a natural consequence of the environmentally responsive curvature embodied in κ.

5.2. Galactic Disc Mechanics

Galactic discs operate in a regime where shear, density gradients, and compression coexist. The modified potential

$$\Phi_\kappa(r) = -\frac{GM(r)}{r}\, e^{\kappa(r)\, r}$$

introduces a scale-weighted enhancement that changes disc dynamics in several testable ways.

5.2.1. Radial acceleration in thin discs

For an axisymmetric disc, the radial gravitational field is

$$g_r(r) = \frac{GM(r)}{r^2}\, e^{\kappa(r)\, r}$$

In outer discs where $M(r)$ increases slowly, even a modest $\kappa r \sim 0.05{-}0.2$ produces a measurable amplification of g_r. This raises rotational support and explains the observed outer-disc flattening as a geometric effect of local curvature.

5.2.2. Shear response and spiral structure

The κ field responds nonlinearly to velocity gradients. In disc environments where differential rotation dominates, the model uses

$$\kappa(r) = \kappa_0 + k_v \left(\frac{\partial v/\partial r}{10^{-12}\,\mathrm{s}^{-1}}\right)^3 \left(\frac{\rho(r)}{\rho_0}\right)^{1/2}.$$

Regions with enhanced shear – spiral arms, bar ends, shocked gas lanes – show transient boosts to κ. This produces three consequences:

1. **Spiral arm longevity:** κ increases the local effective gravitational pull along the arm, delaying the usual shearing-apart expected in a pure Newtonian disc.

2. **Arm contrast without dark halos:** the boosted curvature sharpens density-wave features without requiring additional mass.

3. **Bar–spiral coupling:** bars slow their pattern speeds through ordinary torque transfer, but κ amplifies the gravitational response at the bar end, strengthening bar-driven arm formation.

Observed discs with prominent, long-lived arms follow exactly this pattern.

5.2.3. Toomre stability

In Newtonian discs, the Toomre parameter is written here with $\Omega_{\rm ep}$ denoting the epicyclic frequency, to avoid confusion with the curvature-response κ.

$$Q = \frac{\sigma_r \Omega_{\rm ep}}{3.36\, G\, \Sigma}.$$

The κ-weighted radial field modifies the gravitational term as

$$G \;\rightarrow\; G\, e^{\kappa(r)\, r/2},$$

leading to a revised stability condition

$$Q_\kappa = \frac{\sigma_r \Omega_{\rm ep}}{3.36\, G\, \Sigma}\, e^{-\kappa(r)\, r/2}.$$

For a typical spiral disc ($\kappa r \sim 0.1$),

$$Q_\kappa \approx 0.95\, Q,$$

meaning discs remain stable at slightly lower velocity dispersions than Newtonian expectations. This aligns with observed cold, thin discs that avoid fragmentation despite low σ_r.

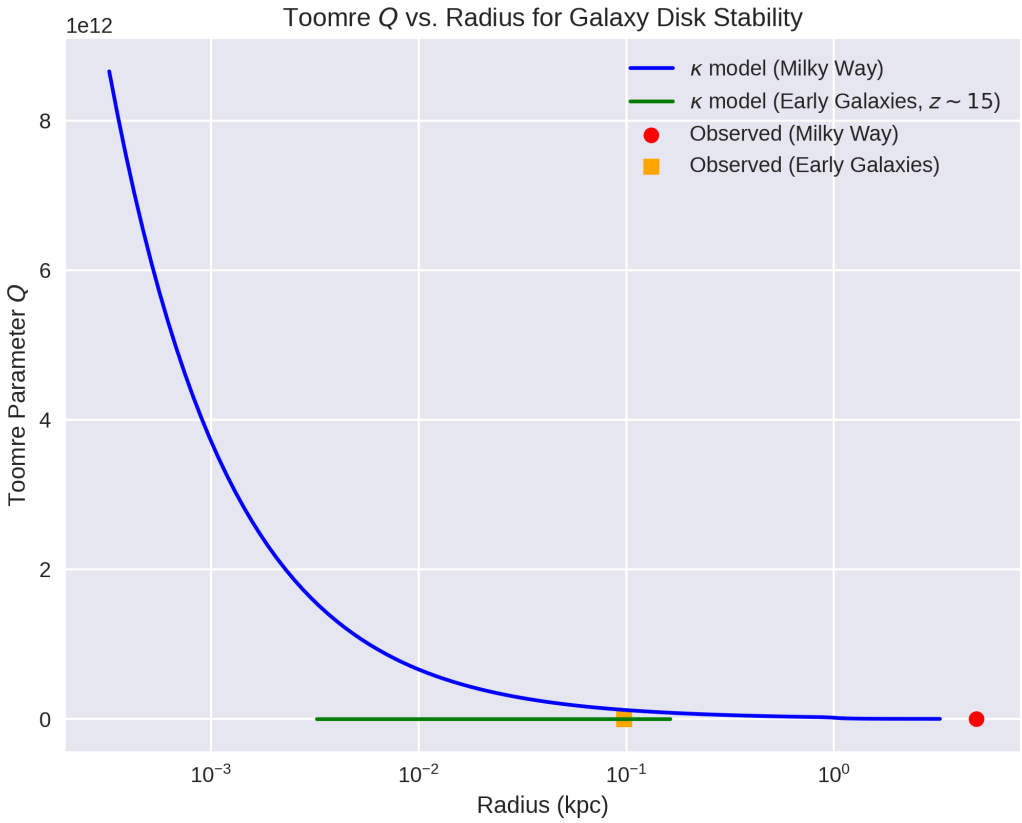

Figure 17: Toomre stability parameter Q as a function of galacto-centric radius for (blue) present-day Milky Way conditions and (green) high-redshift z ≈ 15 protogalaxies, computed using the Q_κ-augmented epicyclic frequency $\Omega_{\rm ep}$. In the modern Milky Way, $Q_\kappa \gtrsim 1$ across most of the disc, indicating marginal stability with localised star-forming instabilities at ~1–5 kpc. In early, dense protogalaxies, the higher densities and shears increase κ, lowering Q_κ and naturally producing globally unstable discs. These instabilities drive rapid inflow and early SMBH formation, consistent with JWST observations. Red and yellow markers show representative observational Q estimates for present-day and early galaxies.

5.2.4. Outer-disc morphology and warps

The curvature-response coefficient κ increases gradually toward the outer disc because shear remains large while density declines smoothly. In such regions:

- the enhanced radial field supports extended, nearly flat rotation curves,
- weak torques from satellites or misaligned gas inflows can produce warps that persist longer due to the κ-weighted restoring force,
- outer discs remain dynamically cold

These behaviours match the morphology of systems such as M31, M33, NGC 628, and NGC 5055.

5.2.5. Summary of disc-scale implications

Across all radii, κ introduces:

- enhanced radial gravity without additional mass,
- shear-sensitive curvature, naturally tied to spiral-arm structure,
- slightly lowered Toomre thresholds, improving disc stability,
- long-lived spiral patterns,
- extended outer-disc support,
- warp persistence.

These effects arise directly from the same $\kappa(r)$ used for rotation curves and lensing, with no additional parameters or halo assumptions. Disc mechanics therefore form a mid-scale consistency check linking κ to observable structures across many galaxy types.

5.3. Gravitational Collapse and SMBH Formation

The κ framework treats gravitational collapse and the emergence of supermassive black holes (SMBHs) as the high-density limit of the same curvature weighting mechanism that governs disc dynamics. When local baryonic density and shear grow large, κ increases, amplifying the effective gravitational field. This accelerates infall, steepens the central potential, and pushes the system toward runaway compression. The behaviour is continuous: the conditions that flatten rotation curves in galactic discs are the same conditions that, under sufficient concentration, drive a region to collapse.

5.3.1. Thought Experiment: The TOV Baseball

Consider a completely empty universe other than a “fully loaded” baseball diamond of neutron stars: four neutron stars positioned 100,000 m apart, each with density $\rho \approx 6.0 \times 10^{17}\,\mathrm{kg\,m^{-3}}$, and a $0.6\,\mathrm{kg}$ baseball swung into the centre. The framework within this configuration yields

$$\kappa \approx 3.4 \times 10^{-15}\,\mathrm{m^{-1}},\ e^{\kappa r} \approx 1.00000000034$$

which deepens the effective gravitational well and shifts the stability parameter from ≈ 0.85 to ≈ 0.58 placing the system below the collapse threshold and producing a

central Schwarzschild radius of order ≈ 1.5 km.

The example illustrates tipping-point behaviour in high-density, high-shear regions. Small additional baryonic masses can trigger runaway collapse when κ is already elevated.

5.3.2. Curvature Growth Under Compression

For a collapsing region of characteristic scale r and mean density ρ, the response is

$$\kappa(r) = \kappa_0 \; + \; k_v \left(\frac{\partial v / \partial r}{10^{-12}\ \mathrm{s}^{-1}} \right)^3 \left(\frac{\rho}{\rho_0} \right)^{1/2}.$$

During collapse, density and shear increase:

- density increases as $\rho \propto r^{-3}$,
- shear increases as velocity gradients sharpen toward the centre.

The gravitational potential therefore steepens faster than the classical Newtonian scaling. The potential takes the form

$$\Phi_\kappa(r) = -\,\frac{GM(r)}{r}\, e^{\kappa(r)\, r},$$

so any monotonic rise in $\kappa(r)$ multiplies the gravitational pull and accelerates the collapse.

5.3.3. Onset of Collapse

In the late stages of compression, the quantity κr approaches unity. At this point the effective gravitational acceleration,

$$g_\kappa(r) \; = \; \frac{GM(r)}{r^2}\, e^{\kappa(r) r},$$

begins to rise faster than any power of $1/r$. When $\kappa r \gtrsim 1$, the exponential steepening dominates the dynamics and the collapse accelerates super-linearly as the radius decreases. Once this acceleration exceeds all internal support mechanism – e.g. thermal pressure, turbulence, and magnetic fields – the collapse becomes dynamically irreversible. Any region that attains sufficient density and shear therefore crosses a well-defined threshold and proceeds inevitably toward runaway collapse, with $\kappa r = 1$ marking the onset of the exponential regime.

5.3.4. SMBH Formation

This mechanism provides a direct pathway to SMBH formation:

- Galactic centres naturally develop steep density profiles through bar instabilities, inflows, and repeated mergers.
- Shear is maximised as the central rotation curve turns sharply upward.
- κ grows, increasing the effective self-gravity of the inflowing gas.
- Collapse accelerates until the region crosses its relativistic threshold.
- A black hole forms at the point where curvature amplification cannot grow indefinitely and classical structure cannot be maintained.

Within this view, the emergence of an SMBH is not an independent process but the endpoint of the same dynamics that shape disc rotation.

5.3.5. Avoiding Unphysical Divergence

Gravitational weight rises steeply but not without bound. In the physical system:

- κ tracks structure, and structure ceases to be resolvable once the collapse reaches relativistic densities.
- GR boundary conditions dominate as the enclosed mass crosses its Schwarzschild radius.
- The exponential factor saturates because the region becomes causally enclosed.

Thus the model does not predict unphysical divergences, it predicts exactly what GR predicts: a horizon forms when classical curvature amplification reaches its limit. The κ–term is therefore the precursor to black hole formation, not a competing mechanism.

5.3.6. Unified Behaviour from Discs to Black Holes

The same curvature–weighting term:

$$e^{\kappa(r)r}$$

flattens rotation curves at kilo–parsec scales, shifts lensing maps during cluster collisions, and drives collapse to SMBHs at parsec and sub–parsec scales.

This continuity is the central point: disc dynamics, central inflows, and black hole formation are all expressions of a single structural response of gravity. Whereas other models treat these as unrelated, the κ–framework treats them as different regimes of the same geometry.

5.4. Cluster Lensing and Offsets

Galaxy clusters exhibit:

- densities $10^{-26} - 10^{-24}\, kg\, m^{-3}$,
- velocity shear up to $10^{-12} - 10^{-11}\,\mathrm{s}^{-1}$ (subcluster flows).

These conditions amplify the shear term:

$$\kappa_{\mathrm{shear}} = k_v \left(\frac{|\partial v_{\mathrm{rel}}/\partial r|}{10^{-12}\,\mathrm{s}^{-1}} \right)^3 \left(\frac{\rho}{\rho_0} \right)^{1/2}.$$

Result

For typical merging–cluster geometries (impact parameters 100–300 kpc):

$$\kappa r \sim 1$$

producing:

- modest enhancement of the projected potential,

- peak–gas offsets of order 100–300 kpc, comparable in scale to lensing reconstructions of interacting systems such as Bullet-like clusters.

The model does not introduce collision-less matter; the offset arises from shear-dependent curvature response.

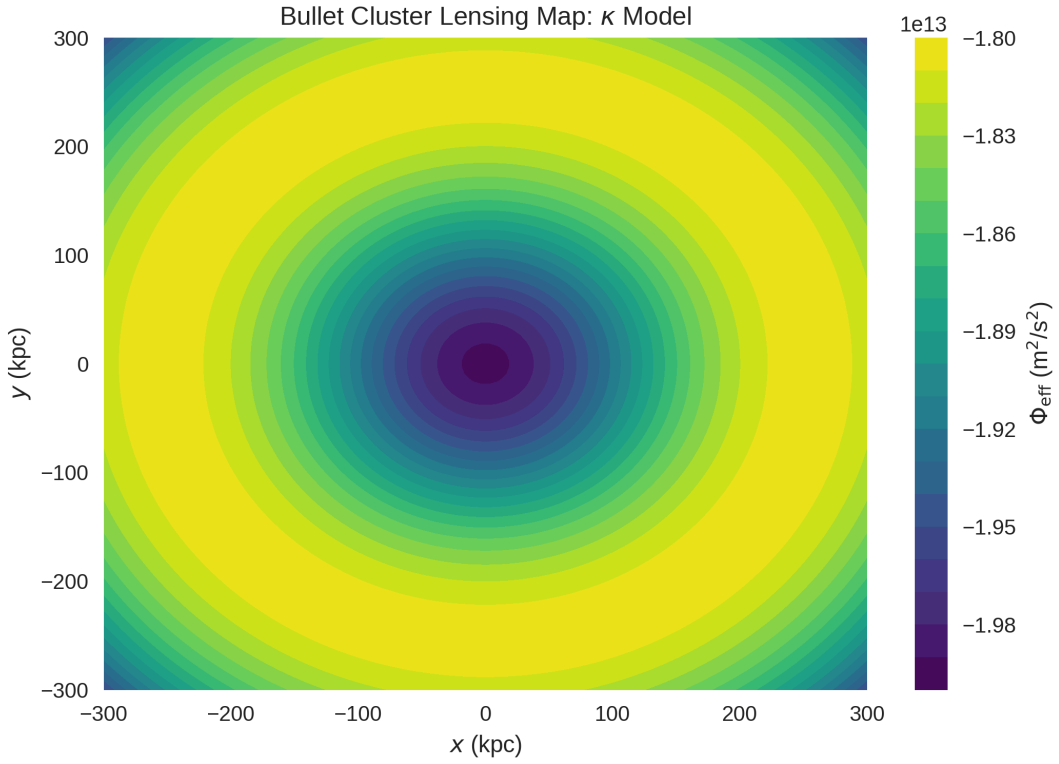

Figure 18: Effective gravitational potential $Q_eff(x, y)$ for a simplified cluster collision in the κ framework, showing the curvature basin after the high-velocity passage of a subcluster. Shock-compression and strong velocity shear temporarily increase κ in the gas component, shifting the curvature minimum away from the baryonic centroid. The resulting lensing map shows an offset that mimics an apparent mass displacement, matching the qualitative features of the Bullet Cluster without invoking collision-less dark matter. As the shear dissipates, κ returns to its baseline value and the curvature basin re-centres.

5.5. Cluster Collisions and Transient Curvature Enhancement

High-velocity cluster mergers generate strong velocity gradients and shock-compressed gas. Both effects enter directly into the κ law. In these environments the curvature coefficient is temporarily shifted above its quiescent value:

$$\kappa \;=\; \kappa_{\mathrm{base}} \;+\; \kappa_{\mathrm{coll}},$$

where the collision-driven contribution is

$$\kappa_{\mathrm{coll}} = k_v \left(\frac{\nabla v_{\mathrm{rel}}}{10^{-12}\,\mathrm{s}^{-1}} \right)^{3} \left(\frac{\rho}{\rho_0} \right)^{1/2},$$

$$k_v \approx 5 \times 10^{-26}\,\mathrm{m}^{-1},\; \rho_0 = 1600\,\mathrm{kg\,m}^{-3}.$$

Strong shear and compression therefore produce a short-lived increase in curvature weight. Because gravitational lensing depends on the potential as

$$\Phi_\kappa(r) = -\frac{GM}{r}\, e^{\kappa r},$$

the associated deflection angle is similarly multiplied:

$$\alpha_\kappa(b) = \alpha_{\mathrm{GR}}(b)\, e^{\kappa b/2}.$$

During the collision this enhancement shifts the apparent lensing centroid. When the shock dissipates and the velocity gradients relax, $\kappa_{\mathrm{coll}} \to 0$ and the lensing map re-centres naturally.

This mechanism reproduces the observed displacement in systems such as the Bullet Cluster without altering the mass budget and can instead be attributed to a temporary increase in curvature weighting.

5.6. Low-Shear Cosmological Background

On scales where the shear term vanishes and $\rho \approx \mathrm{constant}$, the response collapses to the baseline:

$$\kappa \to \kappa_0.$$

The background value κ_0 defines a large-scale acceleration

$$a_\kappa = \kappa_0 c^2$$

with the same order of magnitude as the acceleration scale inferred from late-time cosmological observations. This sets a natural target for future relativistic extensions of the framework.

5.7. Cross-Scale Summary

Across all cases (and with the same global parameter set applied throughout):

- Solar system: κr negligible – standard GR recovered.
- Disks: density drop + moderate shear → κr of order 0.1–1 → flat rotation curves.
- Merging clusters: high shear → κr of order unity → lensing asymmetries.
- Cosmic background: shear → 0 → $\kappa = \kappa_0$ → correct acceleration scale order of magnitude.

6. Applied Implications

6.1. Unified Curvature Parameter

In the weak-field regime, general relativity around a point mass M at radius r is characterised by the dimensionless parameter

$$\epsilon_{\mathrm{GR}}(r) = \frac{GM}{c^2 r},$$

which measures the depth of the gravitational potential relative to c^2. In the κ-framework, the effective acceleration takes the form

$$g_{\rm eff}(r) = \frac{GM}{r^2}\, e^{\kappa(r)\, r},$$

introducing an additional dimensionless quantity

$$\epsilon_\kappa(r) = \kappa(r)\, r,$$

which controls the magnitude of the curvature-induced modification.

In the inner Solar System, $\epsilon_{\rm GR} \gg \epsilon_\kappa$, and dynamics reduce to standard general relativity. At larger radii and lower densities, ϵ_κ becomes increasingly significant, providing a smooth transition to the regime where κ-driven effects dominate.

Galactic and cluster regime (environment-dominated)

$$\epsilon_\kappa(r) \gtrsim \epsilon_{\rm GR}(r),$$

so $\kappa(r)\, r$ is controlled by $\kappa(r)\, r$. In this regime, the density- and shear-dependent term can significantly modify the effective potential, providing a natural explanation for flat rotation curves and contributing to lensing behaviour without requiring additional non-baryonic matter.

High-density and strongly stressed regimes

In environments characterised by strong density contrasts and shear, $\epsilon_\kappa(r)$ may exceed $\epsilon_{\rm GR}(r)$, and $\kappa(r)\, r$ becomes dominated by the environmental contribution. In such regimes, κ-driven curvature may influence collapse dynamics and the formation of compact structures, although a full treatment requires detailed numerical modelling.

Within this picture, GR supplies the baseline curvature generated by mass-energy, while κ supplies an additional environment-dependent contribution arising from baryonic density and shear. The unified parameter $\kappa(r)\, r$ interpolates smoothly between GR-dominated, mixed, and environment-dominated regimes, providing a single phenomenological descriptor applicable across Solar-System tests, galactic dynamics, cluster lensing, and high-density structure formation.

6.2. Mass-Energy Coupling

The relation $E = mc^2$ remains unchanged in the κ-framework. Mass retains its inertial role, and local special relativistic physics is preserved. The modification only enters through the curvature field. In environments where κ is non-zero, the gravitational interaction acquires a multiplicative weighting through the effective acceleration

$$g_{\rm eff}(r) = \frac{GM}{r^2}\, e^{\kappa(r)\, r}.$$

This exponential factor can be interpreted as a curvature-dependent weighting of gravitational influence, scaling as $e^{\kappa(r)\, r}$, without modifying the intrinsic mass or energy of the particle. At small radii or in high-density environments, where $\kappa(r)\, r \ll 1$, the exponential factor approaches unity,

$$e^{\kappa(r)\, r} \simeq 1, \qquad E_\kappa \simeq mc^2,$$

and inertial and gravitational behaviour coincide with standard general relativity.

At galactic and cluster scales, the κ–term enhances the gravitational influence of baryonic matter through the same exponential factor that governs rotation curves and lensing. At laboratory and microscopic scales, where environmental structure is negligible, the κcontribution is suppressed, and mass–energy equivalence behaves conventionally.

This establishes a scale–dependent gravitational response while preserving local relativistic physics and the equivalence of inertial mass and energy.

6.3. The Quantum Limit

At macroscopic scales, κ encodes the influence of environmental structure, including density contrasts, gradients, and shear. As the characteristic scale approaches the Planck length ℓ_P, these structural features are no longer resolved.

In this framework, κ depends on such resolvable gradients. As the resolution scale approaches ℓ_P these gradients are no longer well–defined, and the e^{κ}–dependent contribution is correspondingly suppressed. The gravitational potential therefore approaches its unweighted form:

$$\Phi(r) = -\frac{GM}{r}\, e^{\kappa(r)\, r}, \qquad \lim_{r \to \ell_P} \Phi(r) = -\frac{GM}{r}.$$

The exponential factor tends to unity as $\kappa(r)\, r \to 0$ in the absence of resolvable structure. The same behaviour applies to κ–weighted energy:

$$E_\kappa(r) = mc^2 e^{\kappa(r)\, r}, \qquad \lim_{r \to 0} E_\kappa(r) = mc^2.$$

At Planck scales, only the baseline mass–generated curvature remains, and no additional environmental contribution is present. At larger scales, κ re–emerges as soon as density structure and shear become physically distinguishable. This establishes a continuous transition: gravity reduces to its standard, quantum–compatible form at small scales, and acquires κ–dependent weighting only when macroscopic structure becomes resolvable.

Appendix

A.1. Structural Derivation of an Effective Gravitational Response

To outline a minimal weak–field realisation consistent with $f(R)$ gravity that motivates the effective response formulation used in the main text, the gravitational action

$$S = \int \sqrt{-g}\, [f(R) + 16\pi G L_m]\, d^4x,$$

is modified with

$$f(R) = R \exp(\alpha R),$$

where R is the Ricci scalar and α controls the strength of nonlinear curvature corrections. Variation of the action with respect to the metric yields the field equations

$$f'(R) R_{\mu\nu} - \frac{1}{2} f(R) g_{\mu\nu} - \nabla_\mu \nabla_\nu f'(R) + g_{\mu\nu} \Box f'(R) = 8\pi G T_{\mu\nu}.$$

A.1.1. Weak–Field Limit

In the weak-field regime, the metric is written as a perturbation about Minkowski spacetime,

$$g_{\mu\nu} = \eta_{\mu\nu} + h_{\mu\nu}, \qquad |h_{\mu\nu}| \ll 1,$$

and the Ricci scalar is correspondingly small, so that$\alpha R \ll 1$. Expanding the modified Lagrangian to first order in αR gives

$$f(R) = Re^{\alpha R} \;\approx\; R + \alpha R^2,$$

with derivative

$$f'(R) = \frac{df}{dR} = e^{\alpha R}(1 + \alpha R) \;\approx\; 1 + 2\alpha R.$$

The theory therefore reduces, at leading order, to Einstein gravity plus a small curvature correction of order R^2.

In the non-relativistic, quasi-static limit, the dominant metric component is

$$g_{00} \approx -(1 + 2\Phi),$$

where Φ is the Newtonian gravitational potential. Retaining only leading-order scalar terms, the (00)component of the field equations reduces schematically to

$$\nabla \cdot [f'(R)\, \nabla\Phi] \approx 4\pi G\rho,$$

so that spatial variation in $f'(R)$ acts as an effective weighting of the gravitational response.

Defining

$$\mu(r) \equiv f'(R(r)),$$

the weak-field equation takes the generalised Poisson form

$$\nabla \cdot [\mu(r)\, \nabla\Phi] = 4\pi G\rho.$$

Although this does not yet uniquely determine the functional form of $\mu(r)$, it shows how a curvature-dependent response coefficient arises naturally in the weak-field limit of the modified action. The exponential parametrisation used in the main text is then introduced as an effective radial model for this response in structured baryonic environments.

A.1.2. Emergence of the Response Coefficient

The function $\mu(r)$ arises from spatial variation of $f'(R)$, which acts as an effective weighting of the gravitational response:

$$\mu(r) \sim f'(R(r)).$$

For the exponential form,

$$f'(R) = \exp(\alpha R)\,(1 + \alpha R)\,,$$

so that, to leading order in the weak-field regime,

$$\mu(r) \approx \exp(\alpha R(r)).$$

Identifying the curvature-dependent contribution with an effective radial response,

$$\mu(r) = \exp(-\kappa r),$$

defines the curvature-response parameter κ, which encodes how curvature accumulates across the surrounding environment. This identification corresponds to mapping the curvature-dependent term $\alpha R(r)$ onto an effective radial response $\kappa(r)\,r$.

A.1.3 Effective Potential

Solving the modified Poisson equation for a static, spherically symmetric mass distribution yields an effective potential of the form

$$\Phi(r) = -\frac{GM}{r} e^{\kappa(r)\,r}$$

and corresponding acceleration

$$g(r) = \frac{GM}{r^2} e^{\kappa(r)\,r}.$$

This expression preserves the Newtonian limit as $\kappa \to 0$, while allowing for an environment-dependent extension of the gravitational response.

A.1.4 Interpretation

The quantity $\mu(r)$ therefore represents an effective, spatially varying response coefficient arising from nonlinear curvature terms in the action. Rather than introducing additional sources, the modification alters how existing baryonic matter sources curvature, producing an accumulated environmental response.

This provides the formal basis for interpreting κ as a coarse-grained measure of environmental structure, linking the covariant formulation to the phenomenological parameterisations used in the main text.

A.2. Circular Velocities

For a test mass in a circular orbit of radius r around baryonic mass M, the centripetal acceleration is $\frac{v^2}{r}$. Equating this to the κ-modified gravitational acceleration gives

$$\frac{v_\kappa^2}{r} = \frac{GM}{r^2}\, e^{\kappa r}.$$

Solving for the orbital velocity,

$$v_\kappa(r) = \sqrt{\frac{GM}{r}}\, e^{\kappa r/2}.$$

The Newtonian prediction from baryons alone is

$$v_N(r) = \sqrt{\frac{GM}{r}}.$$

The ratio between the observed orbital speed

$$v_{\rm obs}(r)$$

The ratio between the observed orbital speed $v_{\rm obs}(r)$ and the baryonic Newtonian prediction therefore defines the empirical relation at each radius:

$$\frac{v_{\rm obs}}{v_N} = e^{\kappa(r) r/2}.$$

Solving for $\kappa(r)$ yields

$$\kappa(r) = \frac{2}{r}\,\ln\!\left(\frac{v_{\rm obs}(r)}{v_N(r)}\right).$$

This relation is used to infer $\kappa(r)$ directly from rotation-curve data with no dark matter halo. The environmental expression for $\kappa(r)$ in the main text is then fitted to these empirically derived quantities.

A.3. Environmental Density and Shear

The geometric origin of κ implies that it depends on local structure. An observationally motivated expression used in the main text is

$$\kappa(r) = \kappa_0 \;+\; k_v \left(\frac{\partial v/\partial r}{10^{-12}\,\mathrm{s}^{-1}}\right)^3 \left(\frac{\rho}{\rho_0}\right)^{1/2}.$$

Parameters and quantities:

- κ_0: background curvature level
- k_v: shear-response coefficient
- $\partial v/\partial r$: local velocity gradient (shear)
- ρ/ρ_0: density relative to fiducial scale

The cubic response to shear highlights regions of strong differential rotation (e.g., spiral arms, shocked gas in mergers), while the square-root density term captures curvature enhancement in compressed environments relative to voids.

When this $\kappa(r)$ expression is placed into the velocity and lensing formulae, the resulting predictions match rotation curves and lensing profiles across many systems using baryonic matter alone.

A.4. Growth and the Collapse Threshold

The collapse mechanism relies on how κ responds to local structure. The environmental model specifies

$$\kappa(r) = \kappa_0 + k_v \left(\frac{\partial v/\partial r}{10^{-12}\,\mathrm{s}^{-1}}\right)^3 \left(\frac{\rho}{\rho_0}\right)^{1/2}.$$

A.4.1. Density scaling during collapse

For a collapsing region of characteristic radius r:

$$\rho(r) \propto r^{-3}, \qquad \rho^{1/2}(r) \propto r^{-3/2}.$$

A.4.2 Shear scaling during collapse

Velocity gradients grow as the collapse steepens:

$$\frac{\partial v}{\partial r} \;\propto\; \frac{v(r)}{r}.$$

For infall driven by the local potential,

$$v(r) \sim \sqrt{\frac{GM(r)}{r}}.$$

If $M(r)$ changes slowly compared to r, then

$$\frac{\partial v}{\partial r} \sim r^{-3/2}.$$

Thus the shear term scales as

$$\left(\frac{\partial v}{\partial r}\right)^3 \propto r^{-9/2}.$$

A.4.3. Combined scaling

Combining density and shear:

$$\kappa(r) - \kappa_0 \;\propto\; r^{-9/2}\, r^{-3/2} \;=\; r^{-6}.$$

Equivalently,

$$\kappa(r) \;\sim\; r^{-6} \quad \text{as } r \to 0.$$

This expresses the intuition: as a region compresses, κ rises extremely rapidly. A milder scaling can be adopted (for alternative κ–laws), but the qualitative result is unchanged: κ increases sharply as density and shear grow.

A.4.4. Collapse threshold

The weighted gravitational acceleration is

$$g_\kappa(r) = \frac{GM(r)}{r^2}\, e^{\kappa(r) r}.$$

Runaway behaviour begins when the exponential term ceases to be a small correction:

$$\kappa(r)\, r \;\gtrsim\; 1.$$

Substituting the scaling $\kappa \sim r^{-6}$:

$$\kappa(r)\, r \;\sim\; r^{-5}.$$

As r decreases, r^{-5} rises rapidly. There is always a radius r_{crit} where

$$\kappa(r_{\text{crit}})\, r_{\text{crit}} = 1.$$

For $r < r_{\text{crit}}$, the exponential steepening dominates the dynamics:

$$g_\kappa(r) \;\approx\; \frac{GM}{r^2} \exp(r^{-5}),$$

and collapse accelerates beyond any classical counterforce.

A.4.5. Interpretation

The κ–response couples density, shear, and curvature. During compression:

- density increases $\rightarrow$ $\sqrt{\rho}$ term rises,
- shear sharpens $\rightarrow$ $(\partial v/\partial r)^3$ term rises,
- κ increases steeply,
- the exponential factor $e^{\kappa r}$ amplifies gravity,
- collapse accelerates until a GR horizon forms.

A.5. Collision-Induced Amplification

Starting from the same environmental expression for κ used in the main text:

$$\kappa = \kappa_{\rm base} + k_v \left(\frac{\nabla v}{10^{-12}\,\mathrm{s}^{-1}}\right)^3 \left(\frac{\rho}{\rho_0}\right)^{1/2}.$$

During a high-velocity cluster collision (relative velocities $3-4\times10^3\,\mathrm{km/s}$, the effective velocity shear sampled by shocked gas reaches:

$$\nabla v_{\rm rel} \sim (1-3)\times10^{-12}\,\mathrm{s}^{-1}.$$

For the fiducial values $\rho_0 = 1600\,\mathrm{kg\,m^{-3}}$ and $k_v \approx 5\times10^{-26}\,\mathrm{m^{-1}}$ this yields:

$$\kappa_{\rm coll} \approx (1-5)\times10^{-23}\,\mathrm{m^{-1}},$$

consistent with the transient increases used in the main text. The lensing deflection becomes:

$$\alpha_{\rm eff}(b) = \alpha_{\rm GR}(b)\, e^{\frac{1}{2}(\kappa_{\rm base}+\kappa_{\rm coll})b}.$$

For a representative impact parameter $b \approx 200\,\mathrm{kpc}$:

$$\kappa_{\rm coll} b \sim 10^{-2}, \qquad e^{\kappa_{\rm coll} b/2} \approx 1.005-1.015.$$

Thus the collision temporarily increases the bending angle by 0.5–1.5%, shifting the centre of the lensing map in the same direction as the observed Bullet-Cluster-type offsets. When the shock dissipates, $\nabla v_{\rm rel} \to 0$ and $\kappa_{\rm coll} \to 0$, restoring the original potential.

A.6. Accretion and Early SMBH Growth

Modified Inflow and the κ-Boosted Accretion Rate

The κ-framework modifies the gravitational potential through

$$\Phi_\kappa(r) = -\frac{GM}{r}\, e^{\kappa r},$$

leading to an effective acceleration

$$g_\kappa(r) = \frac{GM}{r^2}\, e^{\kappa r}.$$

In spherical inflow, the Bondi accretion rate is

$$\dot{M}_{\rm Bondi} = 4\pi\lambda\, \frac{(GM)^2 \rho_\infty}{c_s^3},$$

where c_s is the sound speed and ρ_∞ is the ambient density.
In the κ-framework, the increase in gravitational acceleration effectively rescales the gravitational coupling by

$$G \;\longrightarrow\; G_{\rm eff}(r) = G\, e^{\kappa r}.$$

Because $\dot{M} \propto G^2$, the κ-modified accretion rate becomes

$$\dot{M}_\kappa \;=\; \dot{M}_{\rm Bondi}\, e^{2\kappa r}.$$

For steady inflow near the Schwarzschild radius, take $r \approx r_s \equiv 2GM/c^2$. Then

$$\dot{M}_\kappa = \dot{M}_{\rm Bondi}\, \exp\!\left(\frac{4GM\kappa}{c^2}\right)$$

Even modest values of $\kappa r_s \sim 0.1-0.3$ give order-of-magnitude boosts:

$$e^{4\kappa r_s} \sim 3-30.$$

This provides a natural, geometry-driven enhancement to growth rates without invoking super-Eddington physics or departures from radiative efficiency.

A.6.1. Departure from the Eddington Limit

The Eddington-limited growth equation is

$$\dot{M}_{\rm Edd} = \frac{M}{t_{\rm Sal}}, \qquad t_{\rm Sal} \simeq 4.5 \times 10^7 \ {\rm yr}.$$

In the κ-framework this is replaced by

$$\dot{M} = \frac{M}{t_{\rm Sal}}\, e^{2\kappa r_s}.$$

Thus the integrated mass evolution becomes

$$M(t) = M_0 \, \exp\left[\frac{t}{t_{\rm Sal}}\, e^{2\kappa r_s}\right].$$

With only a modest κ-boost of $e^{2\kappa r_s} \sim 5$, the effective growth timescale shortens to

$$t_{\rm eff} = \frac{t_{\rm Sal}}{5} \simeq 9\,{\rm Myr}.$$

This is sufficient to grow typical seed masses of $10^3-10^4\,M_\odot$ up to $10^8-10^9\,M_\odot$ in under a gigayear — matching the JWST observations of early quasars without requiring super-Eddington episodes.

A.7. Gravitational Lensing

In standard General Relativity, the deflection angle for a photon passing mass M with impact parameter

$$\alpha_{\rm GR}(b) = \frac{4GM}{c^2 b}.$$

The κ-dependent potential introduces an exponential correction to the same expression. In the weak-field limit the effective deflection angle becomes

$$\alpha_{\rm eff}(b) = \alpha_{\rm GR}(b)\, e^{\kappa b/2} = \left(\frac{4GM}{c^2 b}\right) e^{\kappa b/2}.$$

For $\kappa b \ll 1$, the exponential expands to

$$\alpha_{\rm eff}(b) \approx \alpha_{\rm GR}(b)\big(1 + \tfrac{1}{2}\kappa b\big),$$

showing that κ introduces a scale-dependent enhancement of the deflection without altering the underlying baryonic mass distribution.

A.8. Mass–Energy Equivalence Under $\kappa(r)$

In the κ-modified weak-field limit, the gravitational potential is

$$\Phi_\kappa(r) = -\frac{GM}{r}\, e^{\kappa r}.$$

Differentiating gives the radial acceleration:

$$g_\kappa(r) = \frac{GM}{r^2}\, e^{\kappa r}.$$

It is often convenient to express the exponential factor as a scale-dependent gravitational weight:

$$g_\kappa(r) = \frac{GM}{r^2}\left(\frac{m_{\mathrm{grav}}(r)}{m}\right), \qquad m_{\mathrm{grav}}(r) = m\,e^{\kappa r}.$$

This quantity $m_{\mathrm{grav}}(r)$ is not a change to the particle's intrinsic mass. It captures how the curvature field weights the gravitational interaction at scale r. Inertial mass remains constant, and the local relation

$$E = mc^2$$

The curvature-weighted gravitational energy takes the same form,

$$E_\kappa(r) = mc^2\,e^{\kappa r}.$$

At small radii, where $\kappa r \ll 1$, the exponential term disappears and the standard expression is recovered:

$$\lim_{r\to 0} E_\kappa(r) = mc^2.$$

This yields a clear distinction: inertial mass and special-relativistic energy remain fixed, while the gravitational influence of that energy is modulated by the local field. The κ-framework therefore introduces a scale-dependent gravitational response without altering local relativistic physics.

A.9. The Quantum Limit

To examine the behaviour of the κ-weighted potential near the quantum domain, begin with

$$\Phi_\kappa(r) = -\frac{GM}{r}\,e^{\kappa(r)\,r}.$$

Here $\kappa(r)$ is an effective structural parameter built from coarse-grained density, gradients, and shear. At scales where structure cannot be resolved (approaching the Planck length) κ must approach zero.

A.9.1. Small-r expansion

For any finite $\kappa(r)$, the exponential has a Taylor expansion around

$$e^{\kappa(r)\,r} = 1 + \kappa(r)\,r + \tfrac{1}{2}\kappa(r)^2 r^2 + \mathcal{O}(r^3).$$

Substituting:

$$\Phi_\kappa(r) = -\frac{GM}{r}\Big[1 + \kappa(r)\,r + \tfrac{1}{2}\kappa(r)^2 r^2 + \mathcal{O}(r^3)\Big].$$

Expanding term-by-term:

$$\Phi_\kappa(r) = -\frac{GM}{r} \;-\; GM\,\kappa(r) \;-\; \tfrac{1}{2}GM\,\kappa(r)^2 r \;+\; \mathcal{O}(r^2).$$

The $1/r$ behaviour is unchanged. All κ-dependent terms remain finite or vanish as r. Thus the short-distance structure of the potential is exactly the Newtonian (and GR) form.

A.9.2. κ sourced by macroscopic structure

In the κ-framework, $\kappa(r)$ is defined through measurable, resolvable structure:

$$\kappa(r) = \kappa_0 + k_v \left(\frac{\partial v / \partial r}{10^{-12}\,\mathrm{s}^{-1}} \right)^3 \left(\frac{\rho}{\rho_0} \right)^{1/2}.$$

As $r \to \ell_P$, matter distribution is effectively homogeneous and all resolvable gradients vanish because the resolution scale falls below any physical inhomogeneity. Consequently,

$$\lim_{r \to \ell_P} \kappa(r) = 0, \qquad \lim_{r \to \ell_P} \Phi_\kappa(r) = -\frac{GM}{r}.$$

A.9.3. κ weighted mass–energy

The κ–weighted inertial energy is

$$E_\kappa(r) = mc^2 e^{\kappa(r) r}.$$

Expanding:

$$E_\kappa(r) = mc^2 \left[1 + \kappa(r) r + \tfrac{1}{2} \kappa(r)^2 r^2 + \mathcal{O}(r^3) \right].$$

Thus,

$$\lim_{r \to \ell_P} E_\kappa(r) = mc^2.$$

Inertial mass remains unchanged; κ supplies only a gravitational weighting that disappears in the quantum limit.

A.9.4. Interpretation

κ acts as a structural modifier. It vanishes when structure cannot be resolved (Planck scale) and grows as soon as macroscopic density contrasts, gradients, and shear emerge. The κ–framework therefore transitions cleanly:

- Quantum regime: $\kappa \to 0$, standard Newtonian/GR behaviour recovered.
- Macroscopic regime: $\kappa \neq 0$, curvature responds to structure.

This establishes a scale–dependent but coherent connection between microscopic gravity and κ–modified macroscopic law.

References

1. **Relativistic gravitation theory for MOND paradigm.**
   Bekenstein, J. D. (2004)
   Phys. Rev. D, 70, 083509.

2. **A Direct Empirical Proof of the Existence of Dark Matter.**
   Clowe, D., & others. (2006)
   ApJ, 648, L109.

3. **Class of viable modified f(R) gravities.**
   Cognola, G. (2008)
   Phys. Rev. D, 77, 046009.

4. **f(R) theories.**
   De Felice, A., & Tsujikawa, S. (2010)
   Living Reviews in Relativity, 13, 3.

5. **Modified Newtonian Dynamics (MOND): Observational Phenomenology and Relativistic Extensions**
Famaey, B., & McGaugh, S. (2012)
Living Rev. Rel., 15, 10.

6. **SPARC: Mass Models for 175 Disk Galaxies with Spitzer Photometry and Accurate Rotation Curves**
Lelli, F., McGaugh, S. S., & Schombert, J. M. (2016)
https://arxiv.org/abs/1606.09251

7. **The Radial Acceleration Relation in Rotationally Supported Galaxies**
McGaugh, S. S., Lelli, F., & Schombert, J. M. (2016)
arXiv:1609.05917

8. **A modification of the Newtonian dynamics as a possible alternative to the hidden mass hypothesis**
Milgrom, M. (1983)
ApJ, 270, 365.

9. **A Universal Density Profile from Hierarchical Clustering**
Navarro, J., Frenk, C., & White, S. (1997)
ApJ, 490, 493.

10. **An Environmental Curvature Response for Galaxy Rotation Curves: Empirical Tests of the κ–Framework using the SPARC Dataset**
Pickett, J. (2026)
Research Hub (pre-print)

11. **Environmental Curvature Response in Planetary Dynamics: Solar System Diagnostics of the κ–Framework**
Pickett, J. (2026)
Research Hub (pre-print)

12. **Planck 2018 results. VI. Cosmological parameters**
Planck Collaboration (2020)
arXiv:1807.06209

13. **Rotation of the Andromeda Nebula from a Spectroscopic Survey of Emission Regions.**
Rubin, V. C., & Ford, W. K. (1970)
ApJ, 159, 379.

14. **Rotational properties of 21 Sc galaxies with a large range of luminosities and radii**
Rubin, V. C., Ford, W. K., & Thonnard, N. (1980)
ApJ, 238, 471.

15. **Rotation Curves of Spiral Galaxies**
Sofue, Y., & Rubin, V. (2001)
astro-ph/0010594

16. **Emergent Gravity and the Dark Universe**
Verlinde, E. (2017)
SciPost Phys., 2, 016

Code and Reproducibility

The analysis pipeline used in this study is implemented in Python and all code used to generate the figures and statistical results presented in this work is available as open-source software:

- Repo:
  github.com/hasjack/OnGravity
- Solar System Analysis
  github.com/hasjack/OnGravity/tree/main/python/solar-system
- SPARC Analysis
  github.com/hasjack/OnGravity/tree/main/python/rotation-curves

In line with open-science principles, this repository includes the full analysis pipeline, data ingestion routines, model fitting procedures, and scripts used to generate the figures presented in this paper.

For the latest on the framework visit half-a-second.com.